Chemical Engineering Journal 500 (2024) 156637

Contents lists available at ScienceDirect

Chemical Engineering Journal

journal homepage: www.elsevier.com/locate/cej

Leveraging side-stream sludge fermentation for phosphorus recovery in wastewater treatment systems

Mengqi Cheng, Albert Guisasola *, Juan Antonio Baeza

GENOCOV. Departament d'Enginyeria Química, Biològica i Ambiental. Escola d'Enginyeria. Universitat Autònoma de Barcelona, 08193, Bellaterra, Barcelona, Spain

ARTICLE INFO

Keywords:
Enhanced biological phosphorus removal (EBPR)
Nutrient removal
P-recovery
Side stream EBPR process (S2EBPR)

ABSTRACT

This study proposes the integration of a new P-recovery strategy through the use of a side stream enhanced biological P removal (S2EBPR) process. To evaluate this alternative, a 150 L pilot-scale anaerobic/anoxic/aerobic (A_2O) plant was operated with a side-incorporated reactor (10 or 23 L) to work as an anaerobic side stream sludge fermenter (SSSF). The P removal performance and possible P-recovery under different hydraulic residence time in the SSSF were evaluated. The integration of the SSSF in the A_2O configuration provided an excellent 98 % P-removal and allowed to create in the SSSF a stream with a very high soluble phosphate concentration (up to 196.5 ± 10.9 mgP/L). The supernatant of the wasted activated sludge (WAS) discharged from the SSSF contained as soluble phosphate up to 40 % of the total P input to the plant.

1. Introduction

Phosphorus (P) is a crucial element for biological processes, yet its excessive quantities in aquatic ecosystems results in eutrophication. The global P demand is steadily rising due to population growth and the increased agricultural fertilizers requirements. As a finite resource, concerns about P scarcity have emerged [1]. Some claim that P reserves can stand for at most 300 years [2], while others adopt a more conservative perspective according to the assumption of 'peak phosphorus' [3]. Regardless, there is a consensus on the need to optimize P utilization which includes implementing P-recovery strategy in P cycles. Recovering P from wastewater offers a sustainable approach to reduce reliance on mined P while preventing its excessive discharge into waterways [4]. Studies suggest that approximately 15 – 20 % of the global P demand could be satisfied through P-recovery from municipal wastewater [5,6]. Consequently, developing sustainable and efficient methods for P removal and recovery from wastewater is imperative.

Enhanced biological phosphorus removal (EBPR) is a cost-effective and efficient method for P removal from wastewater compared to chemical precipitation. It necessitates alternating anaerobic and aerobic (or anoxic) conditions to cultivate polyphosphate-accumulating organisms (PAO). PAO can uptake carbon sources, mainly volatile fatty acids (VFA), under anaerobic conditions by using the energy derived from intracellular polyphosphate (poly-P) hydrolysis, glycolysis and tricarboxylic acid cycle to covert VFA as polyhydroxyalkanoates (PHA), which are stored intracellularly [7]. Subsequently, PAO are capable to use the stored PHA as carbon source and energy resource under aerobic/anoxic conditions to grow, replenish internal glycogen reserves and accumulate P as poly-P [8]. One important objective in EBPR systems is to enhance PAO activity and prevent the proliferation of other competitors such as glycogen accumulating organisms (GAO), which do not contribute to the bio–P release/uptake processes [9,10].

However, real/full-scale EBPR systems often face challenges due to low influent carbon source, excessive nitrite/nitrate load from the external recycle or hydraulic shocks [11,12]. Optimizing key operational parameters, such as carbon/nitrogen/phosphorus (C/N/P) ratio [13], dissolved oxygen (DO), sludge retention time (SRT) [14] and properly designed configuration [15], operation [16] and control [17], are crucial for efficient EBPR. To address carbon limitations, external carbon source supplementation [18] or on-site primary/secondary sludge fermentation can be implemented [19]. The side stream enhanced biological P removal (S2EBPR) process integrates a side-stream sludge fermenter (SSSF) into a conventional EBPR configuration, offering an improved EBPR operation by generating additional VFA and reducing external carbon needs [19]. Generally, a proportion (4 % – 30 %) of return activated sludge (RAS) is diverted to the SSSF and its effluent is returned to the mainstream receiving influent [15,20]. S2EBPR can lead to more efficient C/N/P-removal compared to conventional EBPR process and, consequently, the number of full-scale applications of S2EBPR facilities worldwide is increasing [21]. For

* Corresponding author.
E-mail addresses: mengqi.cheng@autonoma.cat (M. Cheng), albert.guisasola@uab.cat (A. Guisasola), JuanAntonio.Baeza@uab.cat (J.A. Baeza).

https://doi.org/10.1016/j.cej.2024.156637

Available online 11 October 2024

instance, a full-scale pilot study proved that both P-removal and denitrification were improved when 100 % of RAS was diverted to the SSSF [19]. Sabba et al. [22] conducted pilot and modelling studies of S2EBPR, showing that the RAS diversion ratio of roughly 20 %-25 % would lead to an optimal P effluent. Lv et al. [23] operated a 44 L lab-scale S2EBPR under 4 different RAS diversion ratios (13.3 %, 10.0 %, 8.0 % and 6.7 %), revealing that RAS diversion ratios above 10.0 % had a negative effect on P-removal performance.

In view of P-recovery, within conventional EBPR processes, the primary opportunity for P-recovery lies in the wasted P-enriched sludge [24]. This sludge typically originates from the external recycle line and exhibits a high poly-P content due to the activity of PAO. While the EBPR process achieves high P removal efficiencies (approximately 90–95 % influent P is incorporated into the sludge), effective P-recovery necessitates additional treatment of the sludge stream aiming to maximize the release of intracellular poly-P from the P biomass [25]. Another potential avenue for P-recovery is in the mainstream line itself [26]. However, it has been pointed out that there is a maximum amount (around 60 %) that can be extracted from the mainstream P configuration without hindering PAO activity [27]. The so-called mainstream P-recovery can enhance P-removal performance even with influents with a relatively low chemical oxygen demand (COD) to P ratio. Compared to sludge-based recovery, mainstream P-recovery offers advantages since the presence of calcium (Ca^{2+}), magnesium (Mg^{2+}), and/or silicate ions in sludge can hinder the transition of P from the solid to liquid phase, leading to significant variations in P-recovery efficiency (0–75 %, [6]).

The previous focus in the P-recovery field has been to generate P-rich supernatant that eases P precipitation and, thus, P-recovery. However, values of 30–70 mg/L are typically reported [28]. There are even less studies focused on P-recovery in a S2EBPR process. Zhu et al. [29] proposed an AAO-SBSPR (anaerobic/anoxic/oxic-sequencing batch side stream P recovery) process for achieving high P-recovery rate (up to 65 %). In this configuration, a controlled portion of the influent carbon substrate was directed to the side stream P-recovery reactor. The impact of P-extraction on the intracellular P content of the mainstream sludge was controlled, enabling stable process operation at high P-recovery rates. Lately, Zhang et al. [30] demonstrated through a 150 L pilot plant that the VFA produced in the SSSF was used *in-situ* for PAO leading to a stream with a high P content (above 100 mg/L), but the potential and stability of this P-recovery process was lack of investigation.

Therefore, this work aims to demonstrate the possibility of using the S2EBPR configuration to aid P recovery. It comprehensively studies different operating conditions of the SSSF reactor to produce a highly enriched P-concentrated stream that can be used for P-recovery, significantly increasing the amount of P recovered compared to other configurations.

2. Materials and methods

2.1. Equipment and operation parameters

S2EBPR (Fig. 1) is a modification of the classical A_2O configuration, the latter consisting of three continuous stirred tank reactors: anaerobic (R1, 28 L), anoxic (R2, 28 L), aerobic (R3, 90 L) and a settler (50 L). An additional SSSF (10/23 L) was integrated to the A_2O plant to collectively form a S2EBPR configuration. The SSSF was a continuous stirred tank reactor that received part of RAS and was operated under anaerobic conditions to promote sludge fermentation. The A_2O reactors were

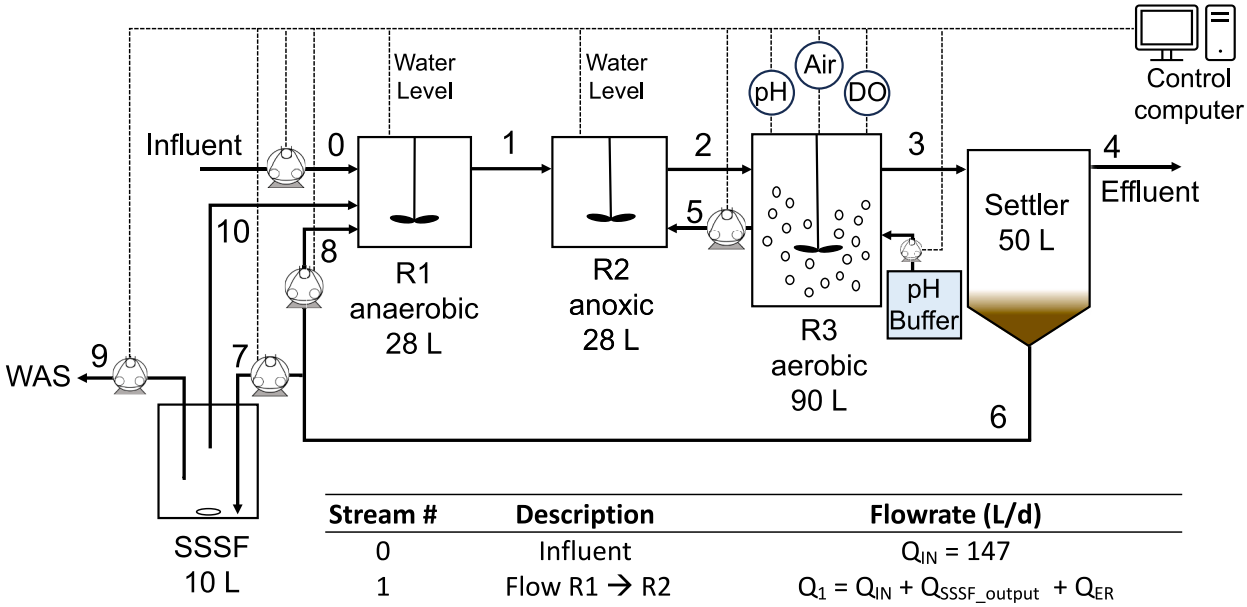

Stream #	Description	Flowrate (L/d)
0	Influent	Q_{IN} = 147
1	Flow R1 → R2	$Q_1 = Q_{IN} + Q_{SSSF\_output} + Q_{ER}$
2	Flow R2 → R3	$Q_2 = Q_1 + Q_{IR}$
3	Flow R3 → Settler	$Q_3 = Q_1$
4	Effluent	Q_{EF} = 144
5	Internal recycle	Q_{IR} = 450
6	Return activated sludge	$Q_{RA} = Q_{ER} + Q_{SSSF\_input}$
7	SSSF_ input	Q_{SSSF_input} = from 4 to 10
8	External recycle	Q_{ER} = 105
9	Waste activated sludge	Q_{WA} = 3
10	SSSF_ output	$Q_{SSSF\_output} = Q_{SSSF\_input} - Q_{WA}$

Fig. 1. Schematic diagram of the S2EBPR configuration implemented in this work.

monitored on-line with DO (HACH CRI6050), pH (HACH CRI5335) and temperature probes (Axiomatic Pt1000) connected to multimeters (HACH CRI-MM44). Data acquisition and process control was performed through the AddControl software (LabWindows CVI, National Instruments) developed in our research group for process monitoring and control [31]. The system was operated at room temperature (22 ± 2 ℃). The flow between reactors, wasted activated sludge (WAS) and RAS was regulated by means of fixed speed peristaltic pumps (Watson Marlow 520-FAM) with timed on-time managed by the AddControl software. The biomass for inoculation was obtained from the municipal wastewater treatment plant (WWTP) of Manresa (Catalonia, Spain).

The plant was operated (Fig. 1) with influent flowrate Q_{IN} = 147 L/d, internal recycle Q_{IR} = 450 L/d, and external recycle Q_{ER} = 105 L/d. The whole experimental period was divided into six operational periods (Table 1), where periods II − VI were used to study the feasible P-recovery from the SSSF. Different SSSF hydraulic residence times (HRT_{SSSF}) were established by adjusting the flowrate of RAS diverted to this reactor (Q_{SSSF_input}). WAS was discharged from the SSSF at Q_{WA} = 3 L/d to maintain the desired SRT (17 to 24 days), but it also contained the P to be recovered. The HRT_{SSSF} was in the range of 1—2.5 days in alignment with previous studies [19,30]. The higher HRT tested of 2.5 days in the 10 L SSSF resulted in Q_{SSSF_input} = 4 L/d, Q_{WA} = 3 L/d and consequently Q_{SSSF_output} = 1 L/d, which was considered to be the lowest flowrate from the SSSF to the anaerobic reactor that could have a significant impact on converting the A_2O configuration to an S2EBPR configuration. The HRT_{SSSF} was adjusted when the plant reached pseudo-steady state, defined as the point at which the P concentration in the SSSF stabilised at around 10 % of its mean value. In the final experimental phase (period VI), a larger SSSF (23 L) was used to investigate the impact of increasing the RAS diversion ratio towards the SSSF (Q_{SSSF_input}) on S2EBPR performance while maintaining a constant HRT_{SSSF}. The pH measured in the SSSF was in the range of 6.1–6.8 during all periods (Fig. S1).

The synthetic plant influent was made by diluting a concentrated solution with a tap water stream to a total flow rate of 147 L/d. The composition of the concentrated solution followed a previous study [25] and is shown in table S1. The influent COD concentration (COD_{IN}) was 600 mg/L, with a COD load (COD_{LOAD}) of 88.5 g/d and a COD ratio of 1:1 of sodium propionate and sodium acetate. The phosphorus in the influent (P_{IN}) was 10 mg P-PO_4^{3-}/L and the load of P (P_{LOAD}) was 1.48 g/d, while the influent ammoniacal nitrogen (N_{INF}) was 40 mg N-NH_4^+/L and the nitrogen load (N_{LOAD}) 5.9 g/d.

The reported SRT in A_2O and S2EBPR configurations was calculated as Eqs. (1) and (2).

$$SRT_{A_2O} = \frac{V_{ANA}\cdot X_{ANA} + V_{ANOX}\cdot X_{ANOX} + V_{AER}\cdot X_{AER}}{Q_{WA}\cdot X_{AER} + Q_{EF}\cdot X_{EF}} \quad (1)$$

$$SRT_{S2EBPR} = \frac{V_{ANA}\cdot X_{ANA} + V_{ANOX}\cdot X_{ANOX} + V_{AER}\cdot X_{AER} + V_{SSSF}\cdot X_{SSSF}}{Q_{WA}\cdot X_{SSSF} + Q_{EF}\cdot X_{EF}} \quad (2)$$

Where V_{ANA}, V_{ANOX}, V_{AER} and V_{SSSF} (L) were the volumes of the anaerobic, anoxic aerobic and SSSF reactors, X_{ANA}, X_{ANOX}, X_{AER} and X_{SSSF} (g/L) their total suspended solids (TSS) concentrations, and X_{EF} (g/L) the TSS in the effluent. Q_{WA} was the WAS flowrate from the aerobic reactor in the A_2O configuration, and from the SSSF for the S2EBPR. Q_{EF} (L/d) was the effluent flowrate.

2.2. Performance indicators

Regarding the removal performance for P, N and COD (P_{REM}, N_{REM} and COD_{REM}, g/d), they were calculated as Eqs. (3)–(5), where P_{DIS_EF}, TN_{DIS_EF}, COD_{DIS_EF} (g/d) are the soluble P, N and COD discharge in the effluent, P_{IN}, N_{IN}, COD_{IN} (g/L) the concentrations of P, N and COD in the influent and P_{EF}, TN_{EF}, COD_{EF} (g/L) the concentrations of soluble P, TN (sum of N-NH_4^+, N-NO_3^- and N-NO_2^-) and COD in the effluent.

$$P_{REM} = P_{LOAD} - P_{DIS\_EF} = P_{IN}\cdot Q_{IN} - P_{EF}\cdot Q_{EF} \quad (3)$$

$$TN_{REM} = N_{LOAD} - TN_{DIS\_EF} = N_{IN}\cdot Q_{IN} - TN_{EF}\cdot Q_{EF} \quad (4)$$

$$COD_{REM} = COD_{LOAD} - COD_{DIS\_EF} = COD_{IN}\cdot Q_{IN} - COD_{EF}\cdot Q_{EF} \quad (5)$$

The fate of N_{LOAD} was calculated with equations (S1-S9) of the Supplementary Information (SI), with i) N_{EFFS} and N_{WASS} as soluble N discharged in the effluent and WAS, ii) N_{EFFB} and N_{WASB} as N in the biomass in the effluent and WAS, iii) N_{LIQUID} as the total soluble N, iv) $N_{BIOMASS}$ as the total N in the biomass, v) N_{EFF} and N_{WAS} as the total nitrogen in the effluent and WAS, and vi) $N_{DENITRIFIED}$ as the N denitrified in form of N_2.

Similarly, the fate of the inlet COD_{LOAD} was calculated with equations (S10-S18) of the SI, with i) COD_{EFFS} and COD_{WASS} as soluble COD discharged in the effluent and WAS, ii) COD_{EFFB} and COD_{WASB} as COD in the biomass in the effluent and WAS, iii) COD_{LIQUID} as the total soluble COD, iv) $COD_{BIOMASS}$ as the total COD in the biomass, v) COD_{EFF} and COD_{WAS} as the total COD in the effluent and WAS, and vi) $COD_{MINERALIZED}$ as COD oxidised as CO_2.

2.3. Chemical analysis

Liquid samples for analysis of soluble phosphate, COD, ammonium, nitrate and nitrite were withdrawn from every reactor almost daily. After the filtration with 0.22 μm filters (Millipore), phosphate was analysed by a phosphate analyser (115 VAC PHOSPHAX sc, Hach-Lange); ammonium concentration by kits (LCK303, 304, Hach); nitrate and nitrite were detected with Ionic Chromatography (DIONEX ICS-2000). COD samples during period III were measured by the multi N/C pharma series equipment (2100S/1, Analytikjena). COD samples during period I, II, IV, V and VI were measured by commercial kits (LCK 314, 714, Hach) and a spectrophotometer (DR3900, Hach-Lange). Sludge samples were withdrawn from the reactors and effluent for the analysis of mixed liquor volatile suspended solids (VSS) and TSS by a heating oven (UF75, Memmert) and a high temperature muffle furnace (12/PR300, Hobersal). The sludge volume index (SVI) was calculated as volume (mL) of sludge from the aerobic reactor after settling for 30 mins over the TSS (g/L) measured on the same day. The analytical methodologies employed have previously been demonstrated to be reliable, and thus no replicates were conducted in general, as the results would be deemed sufficiently robust.

Table 1
Operational conditions for each experimental period.

Period	Day operation	Process	V_{SSSF} (L)	RAS diversion rate to SSSF (%)	HRT_{SSSF} (d)	WAS position	WAS flow (L/d)
I	1–28	A_2O	–	–	–	Aerobic	7
II	29–81	S2EBPR	10	4.8	2	SSSF	3
III	82–141	S2EBPR	10	6.3	1.5	SSSF	3
IV	142–155	S2EBPR	10	9.0	1	SSSF	3
V	156–230	S2EBPR	10	3.8	2.5	SSSF	3
VI	231–293	S2EBPR	23	8.3	2.5	SSSF	3

2.4. P-recovery opportunities

During the S2EBPR process, there were three potential locations for P-recovery: i) aerobic WAS, ii) SSSF effluent or iii) anaerobic WAS. In this study, P-recovery through aerobic WAS was discarded due to the requirement for additional treatment to release intracellular poly-P for efficient P-recovery [25,30]. The P-recovery efficiency from SSSF effluent (PRE_{SSSF}, %) was calculated as Eq. (6), where P_{SSSF} (g/L) referred to the soluble P concentration in the SSSF effluent.

$$PRE_{SSSF}(\%) = \frac{P_{SSSF} \cdot Q_{WA}}{P_{LOAD}} \cdot 100\% \quad (6)$$

The P-recovery efficiency from anaerobic WAS stream (PRE_{ANA}, %) was theoretically calculated assuming the same SRT as in S2EBPR. The theoretical WAS flowrate from anaerobic reactor (Q_{WA_ANA}, L/d) to maintain the current SRT was calculated by Eq. (7). The PRE_{ANA} (%) was calculated according to the P_{ANA} (g/L) concentration as shown in Eq. (8).

$$Q_{WA\_ANA} = \frac{X_{SSSF} \cdot Q_{WA}}{X_{ANA}} \quad (7)$$

$$PRE_{ANA}(\%) = \frac{P_{ANA} \cdot Q_{WA\_ANA}}{P_{LOAD}} \cdot 100\% \quad (8)$$

Visual MINTEQ [32] was then used to simulate the P-recovery potential in WAS stream of period V (HRT_{SSSF} of 2.5 d) under different concentrations of Mg^{2+}, $N\text{-}NH_4^+$ and Ca^{2+} following our previous work [25].

3. Results and discussion

3.1. Long-term performance evaluation of the S2EBPR system

The pilot-scale S2EBPR was operated for 293 days in addition to the first 70 days as A_2O start-up period. The performance of soluble $P\text{-}PO_4^{3-}$, N and COD removal during the experimental period are shown in Fig. 2 and Table 2. Fig. 3 shows the biomass concentration in the mainstream and side stream and biomass status along all periods. During the A_2O operation (Period I), the $P\text{-}PO_4^{3-}$ removal efficiency increased over time up to an average of 85.6 ± 5.4 %.

3.1.1. P dynamics at different HRT_{SSSF}

Once the SSSF was integrated (period II, i.e. 4.8 % of the RAS diverted to the SSSF and HRT_{SSSF} = 2 d), P_{SSSF} (Fig. 2a) showed a first peak after 10 days (day 40) indicating the significant effect of the SSSF on the biomass and leading to a high P-release. This resulted in a slight biomass loss and a lower P_{SSSF} that did not compromise the S2EBPR performance. The P_{SSSF} rose again after mixing conditions were improved (stirring speed was increased from 280 rpm to 300 rpm) and the walls were cleaned. Then, the P_{SSSF} reached an average of 184.3 ± 11.2 mg/L in the last days of period II. The integration of the SSSF resulted in an improvement of PAO activity and P_{ANA} increased from 47.8 ± 4.2 mg/L (Period I, A_2O) to 59.8 ± 6.4 mg/L (Period II), while the effluent P decreased from 0.21 ± 0.08 mg/L to 0.02 ± 0.02 mg/L. That led to a higher P-removal efficiency of 98.6 ± 1.1 % vs 85.6 ± 5.4 %. This extra anaerobic period in the SSSF with continuous VFA production seemed to promote the competitive advantage of PAO over GAO [15]. VFA were rapidly utilized within the SSSF, maintaining a low steady state VFA concentration despite its continuous production.

The HRT_{SSSF} was decreased to 1.5 d in period III (i.e. 6.3 % of the RAS diverted to the SSSF) to better understand the influence of SSSF on S2EBPR performance. It resulted in a decrease in P_{SSSF} (113.4 ± 13.8 mg /L, days 84–109), associated with a sludge bulking event, the cause of which was not determined. The decrease in HRT increased the organic load, which would have triggered the production of excess EPS, resulting in viscous bulking (i.e. non-filamentous bulking) [33]. The diversion of carbon to EPS affects the settleability properties and hinders the P-removal performance of the whole S2EBPR system [23,30]. After manual removal of all floating biomass (day 110), the plant took 11 days to recover the previous biomass levels (Fig. 3), and no additional viscous bulking episodes were detected despite similar operational conditions.

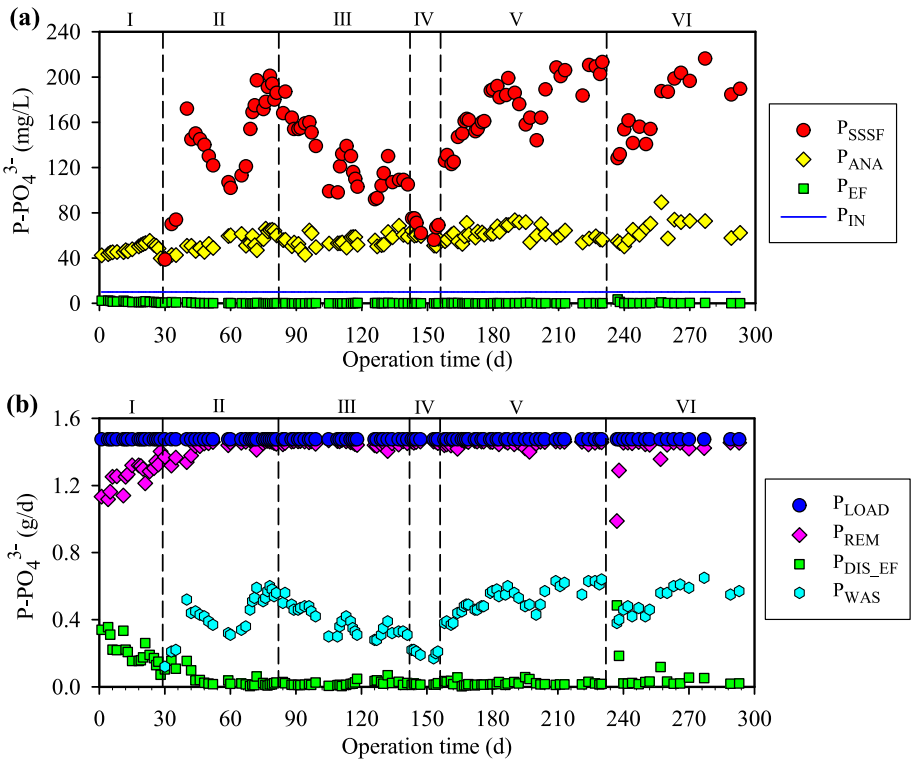

Fig. 2. Phosphorus fate throughout the experimental operation as A_2O (Period I) and S2EBPR (Periods II-VI). (a) Concentrations in the influent and reactors. (b) P load in the input (P_{LOAD}), P load removed (P_{REM}), soluble P load discharged in the effluent (P_{DIS_EF}) and soluble P load in the WAS (P_{WAS}).

Table 2
P, N and COD removal performance for each experimental period at pseudo steady state.

	Period I	Period II	Period III	Period IV	Period V	Period VI
P_{LOAD} (g/d)	1.48 ± 0.00	1.48 ± 0.00	1.48 ± 0.00	1.48 ± 0.00	1.48 ± 0.00	1.48 ± 0.00
P_{SSSF} (mg/L)	–	184.3 ± 11.2	113.4 ± 13.8	67.7 ± 7.0	196.5 ± 10.9	195.5 ± 10.7
P_{ANA} (mg/L)	47.8 ± 4.2	59.8 ± 6.4	56.4 ± 5.2	57.6 ± 4.9	62.1 ± 5.5	69.8 ± 10.5
P_{DIS_EF} (g/d)	0.21 ± 0.08	0.02 ± 0.02	0.03 ± 0.02	0.02 ± 0.00	0.02 ± 0.01	0.04 ± 0.03
Absolute P removal (g/d)	1.26 ± 0.08	1.46 ± 0.02	1.45 ± 0.02	1.46 ± 0.00	1.46 ± 0.01	1.44 ± 0.03
P removal efficiency (%)	85.6 ± 5.4	98.6 ± 1.1	98.3 ± 1.0	98.9 ± 0.3	98.8 ± 0.4	97.9 ± 1.1
N_{LOAD} (g/d)	5.9 ± 0.0	5.9 ± 0.0	5.9 ± 0.0	5.9 ± 0.0	5.9 ± 0.0	5.9 ± 0.0
NH_4^+-N_{SSSF} (mg/L)	–	21.5 ± 1.8	15.8 ± 5.4	7.1 ± 0.7	23.9 ± 2.7	22.4 ± 0.9
TN_{DIS_EF} (g/d)	1.2 ± 0.1	1.4 ± 0.1	1.1 ± 0.3	1.3 ± 0.2	1.6 ± 0.3	1.1 ± 0.5
Absolute N removal (g/d)	4.7 ± 0.1	4.5 ± 0.1	4.8 ± 0.3	4.6 ± 0.2	4.3 ± 0.3	4.8 ± 0.5
N removal efficiency (%)	79.1 ± 1.8	76.6 ± 1.9	81.5 ± 4.6	78.5 ± 2.9	72.9 ± 5.3	81.4 ± 8.4
COD_{LOAD} (g/d)	88.5 ± 0.0	88.5 ± 0.0	88.5 ± 0.0	88.5 ± 0.0	88.5 ± 0.0	88.5 ± 0.0
COD_{SSSF} (mg/L)	–	109.7 ± 12.0	66.4 ± 18.9	85.0 ± 8.5	177.3 ± 19.9	159.3 ± 26.6
COD_{DIS_EF} (g/d)	0.8 ± 0.3	1.1 ± 0.3	4.2 ± 1.0	1.1 ± 0.1	1.0 ± 0.3	0.8 ± 0.1
Absolute COD removal (g/d)	87.7 ± 0.3	87.4 ± 0.3	84.3 ± 1.0	87.5 ± 0.1	87.5 ± 0.3	87.7 ± 0.1
COD removal efficiency (%)	99.1 ± 0.3	98.7 ± 0.4	95.3 ± 1.1	98.8 ± 0.1	98.9 ± 0.3	99.1 ± 0.1

The biomass concentration stabilized over the next 20 days and the SSSF reached an average P_{SSSF} of 113.4 ± 13.8 mg P/L (Fig. 2a). P_{ANA} remained at 56.4 ± 5.2 mg/L and the plant was able to remove 98.3 ± 1.0 % of P. Despite the decrease in P_{SSSF}, the decrease of HRT_{SSSF} did not show a significant effect on the mainstream S2EBPR performance.

The HRT_{SSSF} was then decreased to 1 d (period IV, i.e., 9.0 % of the RAS) to push the system to its limits and, as expected, P_{SSSF} was drastically reduced to 75 mg/L in a single day (day 143) and remained around 67.7 ± 7.0 mg/L for the following 11 days (days 144–155). Again, this change in the SSSF performance did not compromise the overall S2EBPR performance and P_{ANA} remained at 57.6 ± 4.9 mg/L and P-removal efficiency at 98.9 ± 0.3 %. Integration of an SSSF appeared to improve the overall P-removal efficiency over a wide range of SSSF performance levels.

The HRT_{SSSF} was then increased to 2.5 days (period V, i.e. 3.8 % of the RAS diversion), achieving the maximum P_{SSSF} levels of this study of around 200 mg/L. P_{ANA} also increased up to 62.1 ± 5.5 mg/L, without compromising the high P-removal efficiency of 98.8 ± 0.4 %. Finally, period VI was conducted in a 23 L SSSF, maintaining the same HRT_{SSSF} but with a higher RAS diversion ratio (i.e. 8.3 % of the RAS), to reveal the effect of a higher SSSF volume on the S2EBPR performance. It took 23 days to reach steady state (days 235–257), and then stabilized for more than a month. P_{SSSF} reached an average of 195.5 ± 10.7 mg/L, with a high P-removal efficiency of 97.9 ± 1.1 %. These results were similar to those of period V (Table 2), which reveals the positive relation between P concentration and HRT_{SSSF}. independently of the SSSF size.

The major outcome of this almost one-year experimental period in a pilot-scale S2EBPR plant is that a stream with a high P concentration can be generated (about 200 mg P/L), which is extremely suitable for P-recovery (see Section 3.3). The highest P_{SSSF} concentration was 196.5 ± 10.9 mg/L during period V. This is the highest P concentration reported from a side stream RAS fermenter to date. High P values were obtained within a wide range of HRT_{SSSF}. Vollertsen J et al. [34] reported average P concentrations of 28 mg/L and 41 mg/L from side stream hydrolysis tanks in two different full-scale plants. The most recent study by Lv et al. [23] reported an average P of 131.8 ± 4.9 mg/L in the side stream reactor when diverting 8 % of RAS in a 44 L lab-scale S2EBPR. Moreover, we also showed that high P_{SSSF} values were also maintained in the larger SSSF reactor and, thus, that P_{SSSF} is dependent mostly on HRT. On the other hand, a larger SSSF requires a higher RAS diversion ratio for a certain HRT_{SSSF} which may hinder the energy balance of the system.

3.1.2. COD and N removal performance

Independently of the good P-removal performance, Table 2 presents the dynamics of N and COD removal throughout the operational periods. N removal performance in the A_2O period showed an average of 79.1 ± 1.8 %. The SSSF produced a stream with 7 to 24 mg/L N-NH_4^+. The differences in global N removal efficiencies were within the range of experimental deviations observed during pilot plant operation (Table 2), and therefore the SSSF integration did not show any remarkable effect on N removal in this study.

The COD concentration in the SSSF reactor (COD_{SSSF}) increased with the HRT_{SSSF} as the biomass fermentation process was promoted. Not all the COD produced by sludge fermentation was used by PAO and the SSSF effluent contained COD in the range of 60 to 180 mg /L besides the high P concentration. The highest COD_{SSSF} concentration (177.3 ± 19.9 mg/L) was obtained under the highest HRT_{SSSF}. The diversion of organic matter to the mainstream may be of interest if additional COD is required to achieve the targeted nutrient removal, but it must also be considered that the SSSF effluent contains a certain concentration of nitrogen from biomass decay. In the present case, no COD limitation was observed, as the influent COD was sufficiently high.

3.1.3. Biomass evolution

Besides good P, N and COD removal performance, the biomass showed relevant changes during all the periods (Fig. 3, Table S2). The solids in the SSSF were always higher than that in the mainstream due to the use of the concentrated stream from the settler. On average for the 10 L SSSF reactor, VSS_{SSSF} was 1.83 ± 0.12 times VSS_{AER}, and TSS_{SSSF} was 1.72 ± 0.10 times TSS_{AER}. These ratio values are consistent with theoretical calculations based on the input flowrate of the settler and the output flowrate of the settled biomass, around 1.74. Fig. S2(a) represents the ratios VSS_{SSSF}/VSS_{AER} and TSS_{SSSF}/TSS_{AER} with respect to HRT_{SSSF}. A careful analysis reveals some interesting trends (except for the operation at HRT_{SSSF} = 1 d during Period IV, which had a shorter operating time, and the system probably did not reach a steady state). VSS_{SSSF}/VSS_{AER} has a slight trend to decrease with HRT, probably related to the increased biomass decay at higher HRTs. On the other hand, the decreasing trend for TSS_{SSSF}/TSS_{AER} is more pronounced due to the increased poly-P hydrolysis at higher HRT.

The highest biomass concentration in the SSSF was VSS = 5.45 ± 0.37 g/L and TSS = 6.23 ± 0.48 g/L in period VI (HRT_{SSSF} = 2.5 days, table S2). The highest VSS concentration in the mainstream (2.83 ± 0.10 g/L) was observed in period II with the first integration of the SSSF. The VSS/TSS ratio in AER averaged 0.85 ± 0.01 in the A_2O period and decreased to 0.81 ± 0.01 when the SSSF was integrated, indicating higher PAO activity during S2EBPR (Table S2). The VSS/TSS ratio in the SSSF was always higher than that of AER and showed a positive correlation with HRT_{SSSF} (Fig. S2(b)). This trend was clearly related to the anaerobic hydrolysis of poly-P in the SSSF, which increased with

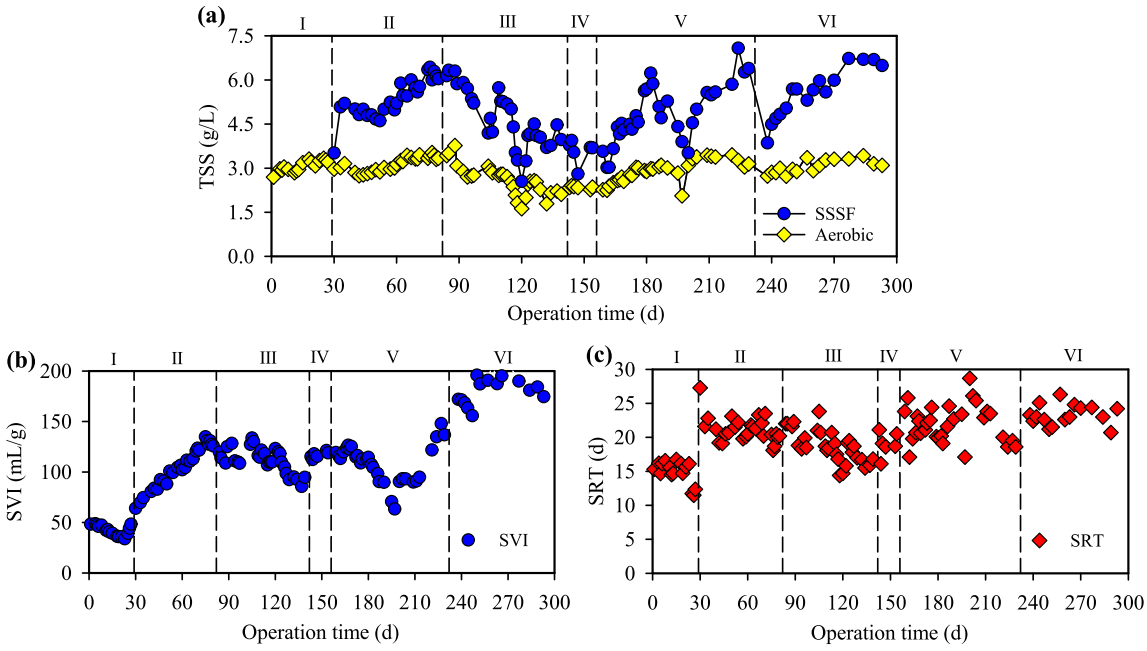

Fig. 3. Evolution of the biomass during different operational periods. (a) TSS concentrations in the SSSF and aerobic tank, (b) sludge volume index of the aerobic reactor (SVI), and (c) sludge retention time (SRT).

increasing HRT_{SSSF}, in agreement with Fig. S2(a).

The findings from our experiments on sludge bulking agree with existing literatures. Previous works identify operational fluctuations (food to microorganism (F/M) ratio, influent loads, nutrient limitations or deficiencies, and low DO concentrations) as key factors in bulking during EBPR [33,35,36]. The integration of SSSF technology may intensify some of these factors, potentially leading to a deterioration in solids settleability. Indeed, we observed a substantial SVI increase (from 42 to around 100 mL/g) after SSSF integration. This SVI value was maintained throughout the operation with the 10 L SSSF and did not compromise plant performance. Moving to a larger SSSF resulted in an increase in SVI up to 190 ± 11 mL/g, probably due to the increased SRT which would have resulted in a lower F/M ratio and a decrease in the percentage of aerobic SRT from 55.2 ± 1.2 to 46.8 ± 0.8 % (Table S2), but it did not hinder EBPR performance. The effluent solids concentration was not significantly affected by the implementation of the SSSF, with values in the range of 0.04 ± 0.02 g/L throughout the experimental period (Fig. S3).

The addition of the SSSF increased the overall amount of biomass in the plant compared to the A_2O configuration, resulting in a higher SRT with a fixed Q_{WA} (Table S2). The SRT with the A_2O configuration was 14.9 ± 1.7 d (period I) and it increased up to 21.9 ± 3.0 d with the SSSF in Period V (HRT_{SSSF} = 2.5 d). With the larger SSSF (23 L), the SRT increased again to 23.4 ± 1.4 d (HRT_{SSSF} = 2.5 d, period VI) due to both the increase of VSS and the reactor volume.

3.2. Mass balances

3.2.1. Phosphorus mass balance

The P mass balance was calculated based on the flowrate and the average $P\text{-}PO_4^{3-}$ concentration in each unit when the system was at pseudo steady state in each operational period. The P was mostly discharged out of the system in the WAS from SSSF, with a smaller fraction of P in the effluent as soluble phosphate and contained in the suspended solids in this stream. The proportion of P discharged from effluent solids were generally low with longer HRT_{SSSF} due to increased hydrolysis of poly-P (Fig. 4). The present study aimed to investigate the potential applicability of P-recovery strategies within the context of the S2EBPR. Thus, it is essential to know which phase contains a higher load of P as well as its concentration.

A positive correlation was observed between HRT_{SSSF} and the extent of P release in both the anaerobic tank and the SSSF (Fig. S2(c)). The trend of higher P concentration at higher HRT_{SSSF} is unlikely to be maintained and saturation of P concentration would probably be observed at higher HRT.

The high P release in the SSSF was due to the VFA generated in the SSSF via biomass decay/fermentation and subsequently consumed *in-situ* by PAO, since there was a minimal content of soluble P in Q_{SSSF_input} (0.001–0.003 gP/d). A P release of 0.785 g/d was observed in the 10 L SSSF at HRT_{SSSF} of 2.5 days. This amount increased to 1.757 g/d when the 23 L SSSF was used with the same HRT_{SSSF}, since similar P_{SSSF} was obtained but the flowrate and volume were higher. A larger reactor may then cause too much P to be released and the plant ability to uptake all this P could be compromised. In a previous work [30], Q_{WA} was not extracted from the SSSF and hence Q_{SSSF_output} contained a high amount of P that was diverted again to the mainstream. That resulted in a significant rise in the P load and, thus, limitations in the P-removal performance of the S2EBPR system.

The amount of P from the anaerobic to the anoxic reactor varied from 14.63 g/d (992.1 % to the input P load) at a HRT_{SSSF} of 1 day to 17.69 g/d (1198.9 % to the input P load) at a HRT_{SSSF} of 2.5 days and 23 L. This flow comprises all the input P to the anaerobic reactor (i.e. Q_{IN}, Q_{ER} and Q_{SSSF_output}) plus the amount of P released. The amount of P released in the anaerobic reactor relies on the organic load and the PAO activity. As observed, it increased with a higher HRT_{SSSF} because of the enhanced PAO activity, for instance, 12.66 g/d at a HRT_{SSSF} of 1 day to 13.17 g/d at a HRT_{SSSF} of 2.5 days. However, the higher value (15.02 g/d) observed in the case of the 23 L SSSF is most likely due to a higher amount of P coming from the SSSF with the higher Q_{SSSF_output} flowrate (6 L/d) (at the same concentration about 200 mg/L).

3.2.2. Nitrogen mass balance

N discharge can be divided into these three outputs (Table 3): N_{EFF} including soluble N in the effluent (N_{EFFS}) and in the biomass (N_{EFFB}), N_{WAS} including soluble N (N_{WASS}) and in the biomass of the WAS (N_{WASB}), and finally $N_{DENITRIFIED}$ as N_2. When only focusing on the N_{EFFS}, it seems that the addition of SSSF neither improved nor weakened the N removal performance. The SSSF integration provides a key benefit by

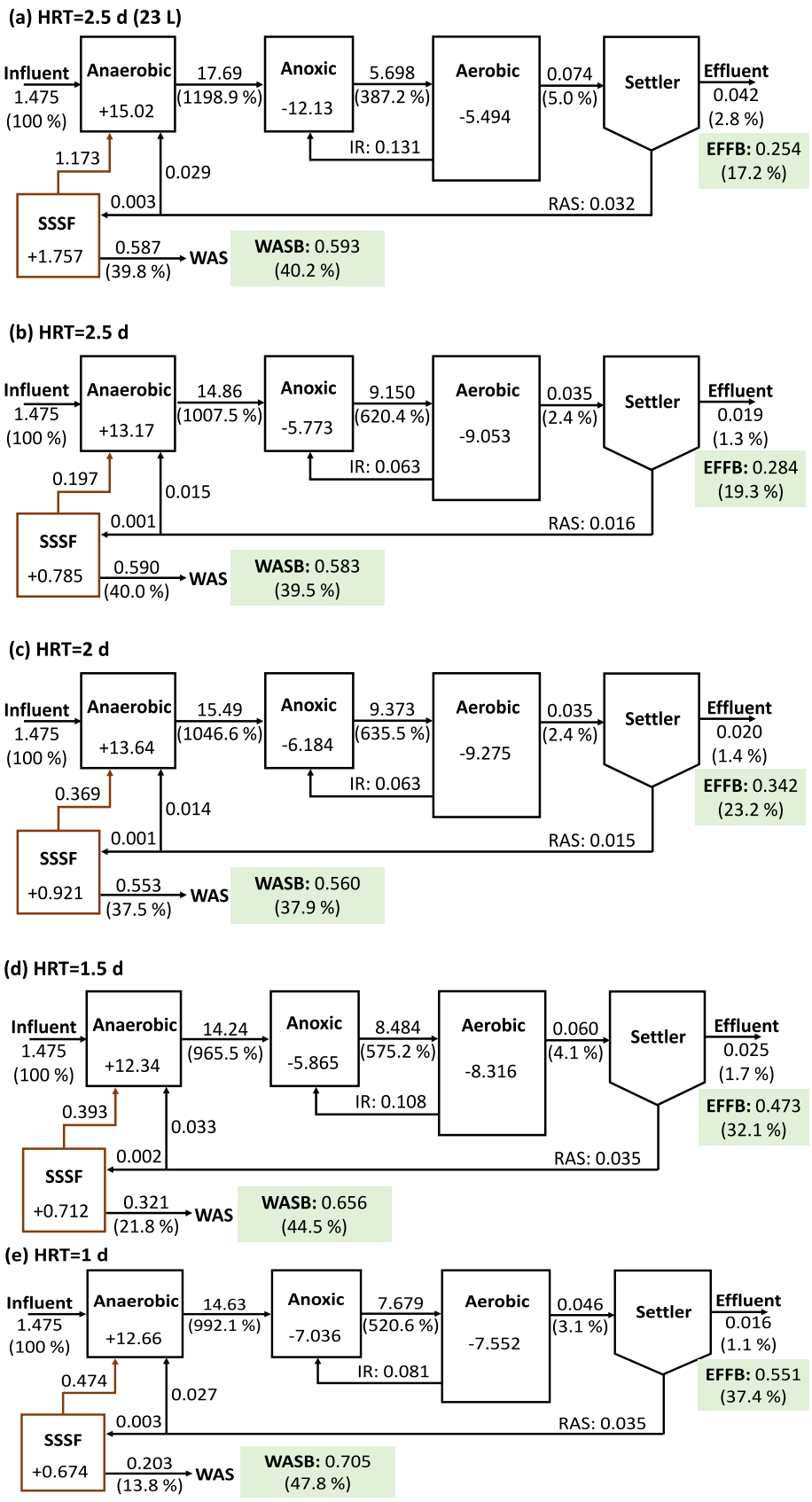

Fig. 4. P mass balance of each operational period at pseudo steady state. Data represent soluble P, except for EFFB and WASB, which refer to the P in the biomass of the effluent and WAS stream. Values without a sign are the P-PO_4^{3-}load (g/d), values with a plus or minus sign represent P-PO_4^{3-}release and P-PO_4^{3-} uptake (g/d). Values in brackets stands for the percentage of P-PO_4^{3-} discharge from each unit compared to the plant P-PO_4^{3-} input (e.g. in (a), the anaerobic 1198.9 % is calculated from 17.69/1.475).

Table 3
Fate of total nitrogen load in A_2O and S2EBPR processes. Please refer to Section 2.2 for the definition of the acronyms.

Period	N_{EFFS} (%)	N_{WASS} (%)	N_{EFFB} (%)	N_{WASB} (%)	N_{LIQUID} (%)	$N_{BIOMASS}$ (%)	N_{EFF} (%)	N_{WAS} (%)	$N_{DENITRIFIED}$ (%)
A_2O	20.9 ± 2.0	1.0 ± 0.1	11.5 ± 2.2	38.3 ± 2.1	22.0 ± 2.0	49.0 ± 4.0	31.8 ± 4.5	39.1 ± 2.8	29.1 ± 5.5
II	23.4 ± 1.9	1.1 ± 0.1	14.7 ± 3.6	34.1 ± 1.9	24.5 ± 1.8	49.1 ± 4.4	38.4 ± 1.9	35.2 ± 2.5	26.4 ± 4.0
III	18.5 ± 4.6	0.8 ± 0.3	14.6 ± 2.7	22.3 ± 4.0	18.9 ± 4.9	36.4 ± 2.9	32.6 ± 3.6	22.7 ± 4.3	44.7 ± 6.1
IV	21.5 ± 2.9	0.4 ± 0.0	14.8 ± 3.5	19.2 ± 2.2	21.9 ± 2.9	32.8 ± 1.7	34.9 ± 4.6	19.8 ± 0.0	45.3 ± 4.6
V	28.7 ± 1.8	1.2 ± 0.1	10.4 ± 1.9	32.1 ± 3.4	29.0 ± 0.6	43.0 ± 3.5	40.2 ± 1.7	31.8 ± 1.8	28.0 ± 2.9
VI	18.6 ± 8.4	1.1 ± 0.0	11.0 ± 2.1	33.6 ± 2.7	19.7 ± 8.4	43.3 ± 1.7	29.8 ± 3.0	33.8 ± 0.9	37.0 ± 7.3

providing a reactor where the nitrate recycled into the SSSF is completely denitrified. This partial nitrate reduction can be critical because high nitrate levels in Q_{ER} can hinder PAO activity in the supposedly anaerobic reactor of the mainstream. This aligns perfectly with the design principles of the S2EBPR, which aims to maintain EBPR despite changing influent conditions.

In the A_2O period, N-removal reached 4.7 ± 0.1 g/d, resulting in a percentage of N in the effluent (N_{EFFS}, %) of 20.9 ± 2.0 % compared to the total N input (5.90 g/d). Consequently, the $N_{BIOMASS}$ (%) remained at 49.0 ± 4.0 % (Table 3). In S2EPBR, the proportion of $N_{BIOMASS}$ (%) tended to decrease particularly when operated with shorter HRT_{SSSF}, for example, 43.0 ± 3.5 % in period V (2.5 d) vs 32.8 ± 1.7 % in period IV (1 d). This is mainly related to the fact that less N-NH_4^+ was released through cell decay/lysis in the SSSF at shorter HRT_{SSSF} [37].

3.2.3. COD mass balance

Similarly, the potential COD discharge outlets are: 1) effluent (COD_{EFF}), as dissolved in the liquid phase (COD_{EFFS}) or contained in the biomass (COD_{EFFB}), 2) WAS (COD_{WAS}), as dissolved in the liquid phase (COD_{WASS}) or contained in the biomass (COD_{WASB}), and 3) mineralized COD ($COD_{MINERALIZED}$). Table 4 summarises the COD mass balance under all operational periods. The additional carbon generated via hydrolysis/fermentation in the SSSF were not considered as extra load to the mainstream since the COD load in Q_{SSSF_output} was always below 1 % of the total COD load.

Table 4 demonstrates near-complete COD removal throughout the experimental study. The effluent in the A_2O period exhibited a low COD_{EFFS} of 0.9 ± 0.3 % of the total influent COD_{LOAD}, and this percentage remained relatively constant during the S2EBPR periods. Regarding COD_{WASS}, it was higher in the S2EBPR operation compared to the A_2O period, but it did not affect the plant performance because Q_{WA} was much lower than Q_{IN}. The COD_{WASB} showed a positive trend with HRT_{SSSF}: 26.0 ± 1.4 % in period II (2 d) vs 14.4 ± 1.8 % in period IV (1 d). This mainly relates to the decrease of the VSS along with the operational HRT_{SSSF} (see section 3.1.3). While reducing WAS solids production generally translates to lower OPEX and a smaller carbon footprint for the WWTP, it can also lead to decreased biogas production if these solids were used for energy recovery, as reported by Zhang et al. [30]. This trade-off arises because lower solids production implies less COD captured in the solids phase. Conversely, S2EBPR exhibited a slightly higher percentage of COD mineralization, likely due to VFA formation in SSSF that enhanced PAO activity. These VFA may be taken up by PAO and subsequently released into the mainstream, leading to increased overall COD utilization.

3.3. Possibilities of P-recovery

S2EBPR presents a novel avenue for P-recovery by facilitating the generation of a high-concentration P stream (i.e. Q_{WA} from the SSSF) while preserving the targeted P-removal efficiency. Compared to previous literature reports, most research has focused on the side stream as the role of producing extra VFA to support low COD/P plants [19,21,38] while only a few works discussed the P concentrations in the side stream reactor. Lv et al. [39] reported their findings on the effect of different RAS diversion ratios on P-removal performance in a S2EBPR and monitored a maximum P concentration about 132 mg/L when the RAS diversion ratio was 8 %. In our work, the highest P concentration reached 200 mg/L, making P-recovery more feasible.

Fig. 5 compares two possible P-recovery scenarios within the S2EBPR framework: 1) the WAS supernatant discharged from the SSSF and 2) the WAS supernatant discharged from the anaerobic tank (calculated as described in section 2.4). P-recovery efficiency in both scenarios were calculated by assuming that all the soluble P could be recovered.

Thus, the estimated PRE_{SSSF} would range from 13.8 % (HRT_{SSSF} = 1 d) to 40.0 % (HRT_{SSSF} = 2.5 d). The proportion of P in the biomass (Fig. S4) exhibited an inverse relationship with HRT_{SSSF}. Specifically,

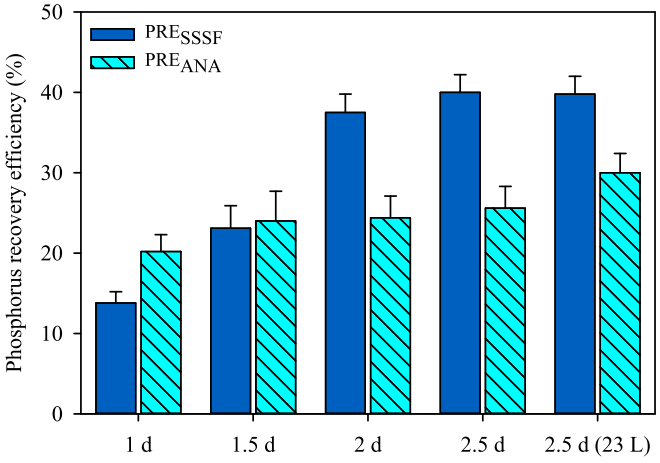

Fig. 5. The potential for P-recovery from the liquid phase of WAS discharged from the SSSF reactor and from the sludge of the anaerobic reactor during each operating period.

Table 4
Fate of the total COD input in A_2O and S2EBPR processes. Please refer to Section 2.2 for the definition of the acronyms.

Period	COD_{EFFS} (%)	COD_{WASS} (%)	COD_{EFFB} (%)	COD_{WASB} (%)	COD_{LIQUID} (%)	$COD_{BIOMASS}$ (%)	COD_{EFF} (%)	COD_{WAS} (%)	$COD_{MINERALIZED}$ (%)
A_2O	0.9 ± 0.3	0.04 ± 0.01	8.9 ± 1.7	29.3 ± 1.7	1.0 ± 0.3	38.2 ± 2.4	10.0 ± 1.4	29.3 ± 1.8	60.7 ± 2.3
II	1.3 ± 0.4	0.4 ± 0.0	11.0 ± 3.0	26.0 ± 1.4	1.6 ± 0.4	36.2 ± 4.3	12.1 ± 4.2	25.3 ± 1.3	62.5 ± 4.9
III	5.0 ± 1.1	0.2 ± 0.1	11.1 ± 2.0	17.0 ± 3.0	5.2 ± 0.5	28.2 ± 2.5	15.8 ± 2.3	17.6 ± 3.3	66.6 ± 2.3
IV	1.2 ± 0.1	0.3 ± 0.0	11.9 ± 2.4	14.4 ± 1.8	1.5 ± 0.1	25.0 ± 1.3	11.4 ± 1.2	15.1 ± 0.0	73.5 ± 1.2
V	1.1 ± 0.3	0.6 ± 0.1	7.9 ± 1.5	24.5 ± 2.6	1.6 ± 0.2	34.1 ± 3.8	9.0 ± 1.3	25.9 ± 3.4	64.3 ± 3.8
VI	0.9 ± 0.1	0.5 ± 0.1	8.4 ± 1.6	25.6 ± 2.1	1.4 ± 0.4	35.1 ± 3.6	10.4 ± 1.5	26.1 ± 2.2	63.5 ± 3.6

the value decreased from 85.2 % at a HRT_{SSSF} = 1 d to 58.8 % at HRT_{SSSF} = 2.5 d. Higher dissolved P concentration in the liquid phase generally facilitates P-recovery because it simplifies the process by potentially eliminating the need for a posttreatment (i.e. poly-P hydrolysis) [40–42]. Consequently, P-recovery performance can be enhanced with extending the HRT_{SSSF}. In this study, increasing the SSSF volume from 10 to 23 L did not significantly affect the PRE_{SSSF} (40.0 % vs 39.8 %) due to the similar soluble P concentrations achieved in both scenarios (196.5 ± 10.9 mg/L in period V, 195.5 ± 10.7 mg/L in period VI, Table 2) and the constant WAS flowrate (Q_{WA} = 3 L/d). An increased Q_{WA} could enhance the P-recovery performance, but it would reduce SRT, and hence the long-term stability of the EBPR process should be experimentally verified.

Significantly, the PRE_{SSSF} of 40 % achieved in this study represents a promising cornerstone for future P-recovery applications. While the maximum P-recovery efficiency observed here falls short of the reported maximum potential range (below 60 %) [43], the SSSF effluent remains highly attractive due to its exceptionally high P concentration, reaching nearly 200 mg/L. This finding represents a significant contribution of this research. Not only does the SSSF integration facilitate the recovery of a high percentage of the influent P, but the increased P content also simplifies the subsequent P recovery steps (for instance, as struvite). Some studies have established minimum P concentration requirements for a techno-economically feasible struvite precipitation. Early works by Barat et al. [43] and Hao et al. [44] suggested a minimum of 25 mg P/L, while subsequent research reported a higher threshold of 50 mg/L [5].

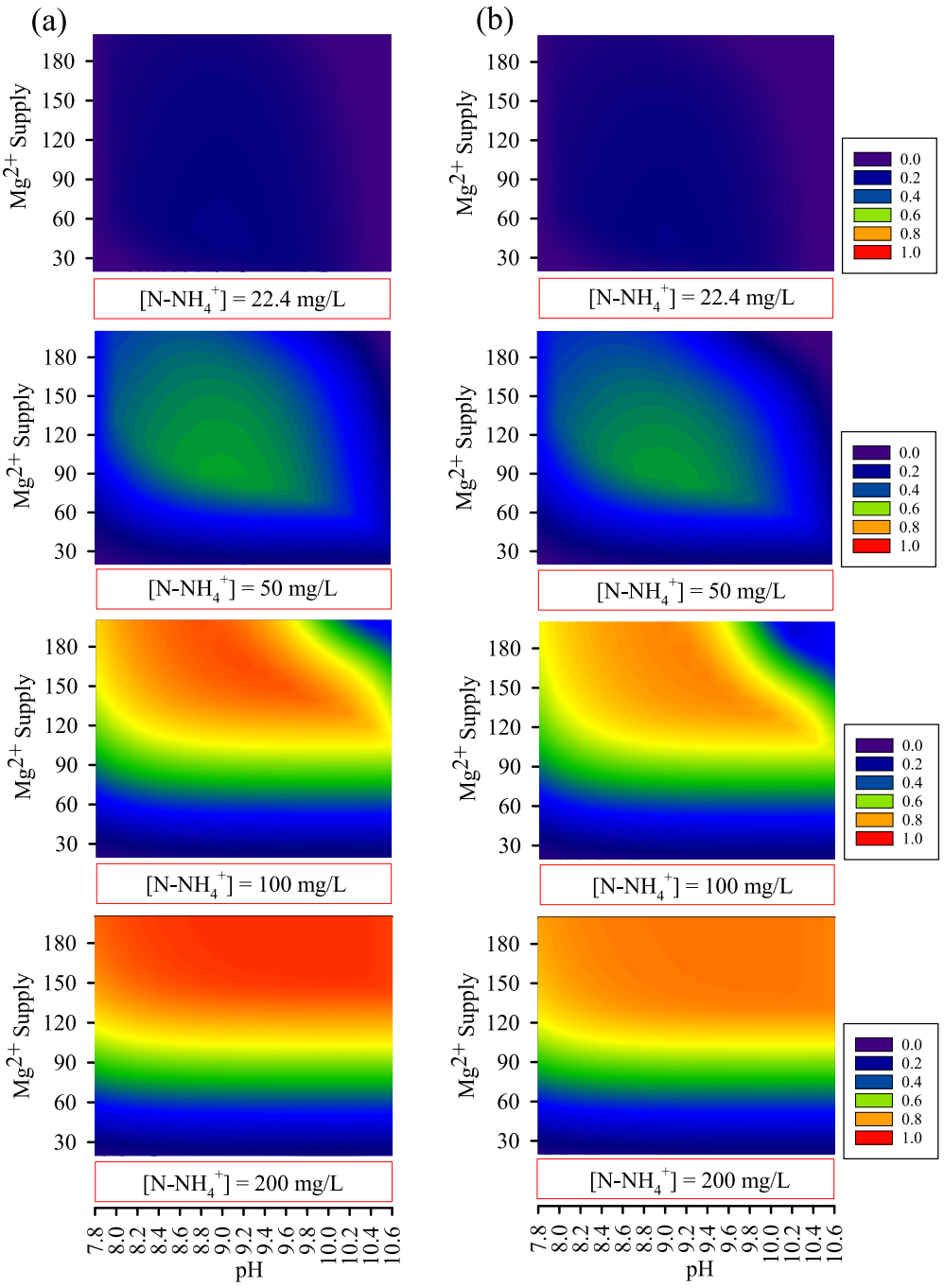

Fig. 6. Simulated fraction of influent $P\text{-}PO_4^{3-}$ precipitated as struvite under varying concentrations of Mg^{2+}, $N\text{-}NH_4^+$ and Ca^{2+} using the WAS stream from HRT_{SSSF} of 2.5 d in the 10 L SSSF for: (a) 20 mgCa/L, (b) 60 mgCa/L.

Further works indicated a need for even higher minimum concentrations, exceeding 100 mg/L for efficient struvite precipitation [4,45]. These values obviously are strongly dependent on the Mg^{2+}, NH_4^+ concentrations and the pH of the effluent. This study achieved P concentrations significantly higher than those previously reported, potentially enhancing the accessibility of P-recovery through struvite precipitation. On the other hand, PAO, even after hydrolysing a significant fraction of their poly-P reserves, still contain a significant fraction of the P load. As illustrated in Fig. S4, approximately 86 % of P remained within the biomass from the outputs of a conventional A_2O process. While this percentage decreased considerably in the S2EBPR under 2.5 d HRT_{SSSF}, a significant fraction around 58 % of P load was still discharged with the biomass, which suggests the need for further treatment to release them for enhanced P-recovery.

Fig. 5 reveals a difference in the P-recovery efficiency from the anaerobic tank (PRE_{ANA}, %) compared to PRE_{SSSF}: PRE_{ANA} values are generally lower. However, an exception occurred during the HRT_{SSSF} of 1 d. This discrepancy can be attributed to comparable P_{ANA} and P_{SSSF} values (mg/L). To maintain the same SRT in the S2EBPR during this period, a higher waste from the anaerobic tank (Q_{WA_ANA} around 5 L/d) was necessary. This increased purge ultimately resulted in a higher PRE_{ANA}.

PRE_{ANA} exhibited a positive correlation with the increasing HRT_{SSSF} and achieved 25.6 ± 2.7 % at a HRT_{SSSF} of 2.5 d in the 10 L reactor, corresponding to an estimated Q_{WA_ANA} around 6 L/d. PRE_{ANA} rose up to 30.0 ± 2.4 % when using the 23 L SSSF under the same HRT_{SSSF}, likely attributed to the increased flowrate entering the anaerobic tank (Table 2). Compared to our previous study evaluating PRE in a typical A_2O plant (PRE_{ANA} = 24.4 %, Q_{WA_ANA} = 7 L/d) [25], the current findings showed an improved PRE_{ANA}, highlighting another positive influence of SSSF on P release even within the mainstream.

Fig. 6 illustrates a theoretical study on the P-recovery opportunities for Q_{WA} at a HRT_{SSSF} of 2.5 d under varying concentrations of Mg^{2+}, N-NH_4^+ and Ca^{2+}. The pH range investigated was 7.8–10.6 in align with previous research [25]. The results indicate that high Ca^{2+} or low Mg^{2+} and N-NH_4^+ levels demoted struvite precipitation. Fig. S5 has shown that the presence of Ca^{2+} likely initiated the formation of hydroxyapatite (HAP) by preferentially binding with PO_4^{3-}, thereby hindering struvite precipitation, which is in agreement with other related research that explored how Ca^{2+} generated competition in both modelling and experimental work [46,47]. Conversely, higher N-NH_4^+ concentration (Fig. 6) promoted struvite formation and elevated the pH range at which greater struvite precipitation occurred. Mg^{2+}, another crucial cation for struvite formation, preferentially reacted with PO_4^{3-} to form $Mg_3(PO_4)_2$ particularly at lower N-NH_4^+ concentrations, as corroborated by the additional simulation results presented in Fig. S6. These findings align with prior studies demonstrating that struvite, under certain conditions, precipitates when PO_4^{3-} concentrations reach 100 mg/L in the presence of N-NH_4^+ [4].

In practice, anaerobic digestion liquor serves as a potential source for NH_4^+ enriched streams. Controlled mixing of these streams can facilitate the precipitation of struvite, promoting its efficient production. In fact, to reach stable precipitation and recovery of struvite, a properly designed control loop based on P concentration and manipulating Mg^{2+} and NH_4^+ addition would be desirable to face the possible fluctuation of these concentrations. Moreover, it is worthy to mention that struvite is only one potential product to recover P as not all WWTPs are EBPR-based. In systems lacking EBPR but implementing chemical precipitation (e.g. A/B or modified Ludzack-Ettinger configuration), vivianite is another viable option, considering the common addition of iron as precipitation agent. However, successful vivianite recovery necessitates a well-designed system, and effective post-separation methods.

4. Conclusions

This work explored the long-term performance of a S2EBPR operated under different HRT_{SSSF}. SSSF integration to a conventional A_2O plant not only increased the P release and uptake activity, but also opened a new scenario for P-recovery. The main conclusions are described as below:

- The S2EPBR showed higher P-removal efficiency up to 98 % than that to 86 % of the A_2O period.
- The P-recovery potential from the SSSF was enhanced with the longer HRT_{SSSF}, yielding around 40 % of the total P input recovered as soluble phosphate from the WAS discharged from the SSSF for HRT_{SSSF} = 2.5 d (10 L SSSF).
- The P mass balance showed that less P was contained in the biomass at the longer HRT_{SSSF}. 58.8 % of the total input P was contained in the biomass phase at HRT_{SSSF} = 2.5 d (10 L SSSF) compared to 85.2 % at HRT_{SSSF} = 1 d (10 L SSSF).
- The SSSF integration does not only facilitate the recovery of a high percentage of the influent P, but the increased P content also simplifies the subsequent P recovery steps (for instance, as struvite).

Further studies to optimize the possibilities of recovering P in this S2EBPR, such as the effect of Q_{WA}, SRT or the relevance between RAS diversion ratio and the reactor size, are required to fully understand the underlying mechanisms of S2EBPR. Meanwhile, a more detailed analysis of COD composition consumption in the process will also be needed to reveal the corresponding PAO activity and denitrification evolution.

CRediT authorship contribution statement

Mengqi Cheng: Writing – original draft, Methodology, Investigation, Formal analysis, Data curation. **Albert Guisasola:** Writing – review & editing, Supervision, Funding acquisition, Formal analysis, Data curation, Conceptualization. **Juan Antonio Baeza:** Writing – review & editing, Supervision, Software, Formal analysis, Data curation, Conceptualization, Methodology, Validation, Visualization.

Declaration of competing interest

The authors declare that they have no known competing financial interests or personal relationships that could have appeared to influence the work reported in this paper.

Acknowledgements

This work was supported by Grant PID2020-119018RB-I00 funded by MCIN/AEI/10.13039/501100011033 (Ministerio de Economía y Competitividad of Spain). Mengqi Cheng would like to thank the financial support from China Scholarship Council (ref 202108310149). The authors are members of the GENOCOV research group (Grup de Recerca Consolidat de la Generalitat de Catalunya, 2021 SGR 515, www.genocov.com).

Appendix A. Supplementary data

Supplementary data to this article can be found online at https://doi.org/10.1016/j.cej.2024.156637.

Data availability

Data will be made available on request.

References

[1] S. Daneshgar, A. Callegari, A.G. Capodaglio, D. Vaccari, The potential phosphorus crisis: Resource conservation and possible escape technologies: A review, Resources 7 (2018), https://doi.org/10.3390/resources7020037.
[2] S.J. Van Kauwenbergh, World Phosphate Rock Reserves and Resources Technical Bulletin IFDC-T-75 (2010).

[3] D. Cordell, S. White, Sustainable phosphorus measures: Strategies and technologies for achieving phosphorus security, Agronomy 3 (2013) 86–116, https://doi.org/10.3390/agronomy3010086.
[4] B.E. Rittmann, B. Mayer, P. Westerhoff, M. Edwards, Capturing the lost phosphorus, Chemosphere 84 (2011) 846–853, https://doi.org/10.1016/j.chemosphere.2011.02.001.
[5] D. Cordell, J.O. Drangert, S. White, The story of phosphorus: Global food security and food for thought, Glob. Environ. Chang. 19 (2009) 292–305, https://doi.org/10.1016/j.gloenvcha.2008.10.009.
[6] S. Petzet, P. Cornel, Towards a complete recycling of phosphorus in wastewater treatment - options in Germany, Water Sci. Technol. 64 (2011) 29–35, https://doi.org/10.2166/wst.2011.540.
[7] A. Oehmen, P.C. Lemos, G. Carvalho, Z. Yuan, J. Keller, L.L. Blackall, M.A.M. Reis, Advances in enhanced biological phosphorus removal: from micro to macro scale, Water Res. 41 (2007) 2271–2300, https://doi.org/10.1016/j.watres.2007.02.030.
[8] A.Z. Gu, A. Saunders, J.B. Neethling, H.D. Stensel, L.L. Blackall, Functionally Relevant Microorganisms to Enhanced Biological Phosphorus Removal Performance at Full-Scale Wastewater Treatment Plants in the United States, Water Environ. Res 80 (2008) 688–698, https://doi.org/10.2175/106143008x276741.
[9] W. Zhao, X. Bi, Y. Peng, M. Bai, Research advances of the phosphorus-accumulating organisms of Candidatus Accumulibacter, Dechloromonas and Tetrasphaera: Metabolic mechanisms, applications and influencing factors, Chemosphere 307 (2022), https://doi.org/10.1016/j.chemosphere.2022.135675.
[10] A.T. Mielczarek, H.T.T. Nguyen, J.L. Nielsen, P.H. Nielsen, Population dynamics of bacteria involved in enhanced biological phosphorus removal in Danish wastewater treatment plants, Water Res. 47 (2013) 1529–1544, https://doi.org/10.1016/j.watres.2012.12.003.
[11] J.L. Barnard, K. Abraham, Key features of successful BNR operation, in, Water Sci. Technol. (2006) 1–9, https://doi.org/10.2166/wst.2006.400.
[12] A. Oehmen, A.M. Saunders, M.T. Vives, Z. Yuan, J. Keller, Competition between polyphosphate and glycogen accumulating organisms in enhanced biological phosphorus removal systems with acetate and propionate as carbon sources, J. Biotechnol. 123 (2006) 22–32, https://doi.org/10.1016/j.jbiotec.2005.10.009.
[13] George Tchobanoglous, Franklin Louis Burton, H. David Stensel, I. Metcalf & Eddy, Wastewater Engineering: Treatment and Reuse, 2014.
[14] U.G. Erdal, Z.K. Erdal, C.W. Randall, The Mechanism of Enhanced Biological Phosphorus Removal Washout and Temperature Relationships, Water Environ. Res 78 (2006) 710–715, https://doi.org/10.2175/106143006X101737.
[15] J.L. Barnard, P. Dunlap, M. Steichen, Rethinking the Mechanisms of Biological Phosphorus Removal, Water Environ. Res 89 (2017) 2043–2054, https://doi.org/10.2175/106143017X15051465919010.
[16] B. Solís, A. Guisasola, X. Flores-Alsina, U. Jeppsson, J.A. Baeza, A plant-wide model describing GHG emissions and nutrient recovery options for water resource recovery facilities, Water Res 215 (2022) 118223, https://doi.org/10.1016/j.watres.2022.118223.
[17] G.S. Ostace, J.A. Baeza, J. Guerrero, A. Guisasola, V.M. Cristea, P.Ş. Agachi, J. Lafuente, Development and economic assessment of different WWTP control strategies for optimal simultaneous removal of carbon, nitrogen and phosphorus, Comput. Chem. Eng. 53 (2013) 164–177, https://doi.org/10.1016/j.compchemeng.2013.03.007.
[18] J. Guerrero, A. Guisasola, J.A. Baeza, Controlled crude glycerol dosage to prevent EBPR failures in C/N/P removal WWTPs, Chem. Eng. J. 271 (2015) 114–127, https://doi.org/10.1016/j.cej.2015.02.062.
[19] D. Wang, N.B. Tooker, V. Srinivasan, G. Li, L.A. Fernandez, P. Schauer, A. Menniti, C. Maher, C.B. Bott, P. Dombrowski, J.L. Barnard, A. Onnis-Hayden, A.Z. Gu, Side-stream enhanced biological phosphorus removal (S2EBPR) process improves system performance - A full-scale comparative study, Water Res. 167 (2019) 115109, https://doi.org/10.1016/j.watres.2019.115109.
[20] P. Devos, A. Filali, P. Grau, S. Gillot, Sidestream characteristics in water resource recovery facilities: a critical review, Water Res. (2023) 119620, https://doi.org/10.1016/j.watres.2023.119620.
[21] A. Onnis-Hayden, V. Srinivasan, N.B. Tooker, G. Li, D. Wang, J.L. Barnard, C. Bott, P. Dombrowski, P. Schauer, A. Menniti, A. Shaw, B. Stinson, G. Stevens, P. Dunlap, I. Takács, J. McQuarrie, H. Phillips, A. Lambrecht, H. Analla, A. Russell, A.Z. Gu, Survey of full-scale sidestream enhanced biological phosphorus removal (S2EBPR) systems and comparison with conventional EBPRs in North America: Process stability, kinetics, and microbial populations, Water Environ. Res 92 (2020) 403–417, https://doi.org/10.1002/wer.1198.
[22] F. Sabba, M. Farmer, Z. Jia, F. Di Capua, P. Dunlap, J. Barnard, C.D. Qin, J. A. Kozak, G. Wells, L. Downing, Impact of operational strategies on a sidestream enhanced biological phosphorus removal (S2EBPR) reactor in a carbon limited wastewater plant, Sci. Total Environ. 857 (2023), https://doi.org/10.1016/j.scitotenv.2022.159280.
[23] T. Lv, D. Wang, J. Hui, W. Cheng, H. Ai, L. Qin, M. Huang, M. Feng, Y. Wu, Effect of return activated sludge diversion ratio on phosphorus removal performance in side-stream enhanced biological phosphorus removal (S2EBPR) process, Environ. Res. 235 (2023), https://doi.org/10.1016/j.envres.2023.116546.
[24] L. Egle, H. Rechberger, J. Krampe, M. Zessner, Phosphorus recovery from municipal wastewater: An integrated comparative technological, environmental and economic assessment of P recovery technologies, Science of the Total Environment 571 (2016) 522–542, https://doi.org/10.1016/j.scitotenv.2016.07.019.
[25] M. Cheng, C. Zhang, A. Guisasola, J.A. Baeza, Evaluating the opportunities for mainstream P-recovery in anaerobic/anoxic/aerobic systems, Sci. Total Environ. 912 (2024) 168898, https://doi.org/10.1016/j.scitotenv.2023.168898.
[26] C. Zhang, A. Guisasola, J.A. Baeza, A review on the integration of mainstream P-recovery strategies with enhanced biological phosphorus removal, Water Res. 212 (2022) 118102, https://doi.org/10.1016/j.watres.2022.118102.
[27] J.A. Baeza, J. Guerrero, A. Guisasola, Optimising a novel SBR configuration for enhanced biological phosphorus removal and recovery (EBPR2), Desalin. Water Treat. 68 (2017) 319–329, https://doi.org/10.5004/dwt.2017.20468.
[28] H. Zou, Y. Wang, Phosphorus removal and recovery from domestic wastewater in a novel process of enhanced biological phosphorus removal coupled with crystallization, Bioresour. Technol. 211 (2016) 87–92, https://doi.org/10.1016/j.biortech.2016.03.073.
[29] Z. Zhu, W. Chen, T. Tao, Y. Li, A novel AAO-SBSPR process based on phosphorus mass balance for nutrient removal and phosphorus recovery from municipal wastewater, Water Res. 144 (2018) 763–773, https://doi.org/10.1016/j.watres.2018.08.058.
[30] C. Zhang, A. Guisasola, A. Oehmen, J.A. Baeza, Benefits and drawbacks of integrating a side-stream sludge fermenter into an A2O system under limited COD conditions, Chem. Eng. J. 468 (2023) 143700, https://doi.org/10.1016/j.cej.2023.143700.
[31] J.A. Baeza, in: Advanced Direct Digital Control (AddControl): Lessons Learned from 20 Years of Adding Control to Lab and Pilot Scale Treatment Systems, Tsinghua University, Beijing (China), 2022, pp. 13–15.
[32] J.P. Gustafsson, Visual MINTEQ 3.1 user guide, (2005).
[33] H.X. Shi, J. Wang, S.Y. Liu, J.S. Guo, F. Fang, Y.P. Chen, P. Yan, Potential role of AHL-mediated quorum sensing in inducing non-filamentous sludge bulking under high organic loading, Chem. Eng. J. 454 (2023), https://doi.org/10.1016/j.cej.2022.140514.
[34] J. Vollertsen, G. Petersen, V.R. Borregaard, Hydrolysis and fermentation of activated sludge to enhance biological phosphorus removal, in, Water Sci. Technol. (2006) 55–64, https://doi.org/10.2166/wst.2006.406.
[35] N. Fan, R. Wang, R. Qi, Y. Gao, S. Rossetti, V. Tandoi, M. Yang, Control strategy for filamentous sludge bulking: Bench-scale test and full-scale application, Chemosphere 210 (2018) 709–716, https://doi.org/10.1016/j.chemosphere.2018.07.028.
[36] X. Lu, G. Yan, L. Fu, B. Cui, J. Wang, D. Zhou, A review of filamentous sludge bulking controls from conventional methods to emerging quorum quenching strategies, Water Res. 236 (2023), https://doi.org/10.1016/j.watres.2023.119922.
[37] H. Lu, J. Keller, Z. Yuan, Endogenous metabolism of Candidatus Accumulibacter phosphatis under various starvation conditions, Water Res. 41 (2007) 4646–4656, https://doi.org/10.1016/j.watres.2007.06.046.
[38] A.B. Lanham, A. Oehmen, A.M. Saunders, G. Carvalho, P.H. Nielsen, M.a.M. Reis, Metabolic versatility in full-scale wastewater treatment plants performing enhanced biological phosphorus removal, Water Res. 47 (2013) 7032–7041, https://doi.org/10.1016/j.watres.2013.08.042.
[39] T. Lv, D. Wang, X. Zheng, J. Hui, W. Cheng, Y. Zhang, Study on specific strategies of controlling or preventing sludge bulking in S2EBPR process, J. Environ. Chem. Eng. 11 (2023), https://doi.org/10.1016/j.jece.2023.110363.
[40] B. Li, I. Boiarkina, W. Yu, H.M. Huang, T. Munir, G.Q. Wang, B.R. Young, Phosphorous recovery through struvite crystallization: Challenges for future design, Sci. Total Environ. 648 (2019) 1244–1256, https://doi.org/10.1016/j.scitotenv.2018.07.166.
[41] V. Carrillo, B. Fuentes, G. Gómez, G. Vidal, Characterization and recovery of phosphorus from wastewater by combined technologies, Rev. Environ. Sci. Biotechnol. 19 (2020) 389–418, https://doi.org/10.1007/s11157-020-09533-1.
[42] P. Kehrein, M. Van Loosdrecht, P. Osseweijer, M. Garfí, J. Dewulf, J. Posada, A critical review of resource recovery from municipal wastewater treatment plants-market supply potentials, technologies and bottlenecks, Environ Sci (camb) 6 (2020) 877–910, https://doi.org/10.1039/c9ew00905a.
[43] R. Barat, M.C.M. van Loosdrecht, Potential phosphorus recovery in a WWTP with the BCFS® process: Interactions with the biological process, Water Res. 40 (2006) 3507–3516, https://doi.org/10.1016/j.watres.2006.08.006.
[44] X.D. Hao, M.C.M. van Loosdrecht, Model-based evaluation of struvite recovery from an in-line stripper in a BNR process (BCFS®), Water Sci. Technol. 53 (2006) 191–198, https://doi.org/10.2166/wst.2006.092.
[45] K.S. Le Corre, E. Valsami-Jones, P. Hobbs, S.A. Parsons, Phosphorus recovery from wastewater by struvite crystallization: A review, Crit. Rev. Environ. Sci. Technol. 39 (2009) 433–477, https://doi.org/10.1080/10643380701640573.
[46] B. Li, I. Boiarkina, B. Young, W. Yu, Quantification and mitigation of the negative impact of calcium on struvite purity, Adv. Powder Technol. 27 (2016) 2354–2362, https://doi.org/10.1016/j.apt.2016.10.003.
[47] S.-H. Lee, B.-H. Yoo, S.J. Lim, T.-H. Kim, S.-K. Kim, J.Y. Kim, Development and validation of an equilibrium model for struvite formation with calcium co-precipitation, J. Cryst. Growth 372 (2013) 129–137, https://doi.org/10.1016/j.jcrysgro.2013.03.010.